Inductive Effects in Ruthenium-Modified Amino Acids

Bernd Geißer,[a] Thomas Skrivanek,[b] Ute Zimmermann,[b] Derk J. Stufkens,[c] and Ralf Alsfasser*[a]

Keywords: Bioinorganic chemistry / Amino acids / Luminescence / Ruthenium

Emission spectroscopy has been used to probe and quantify electronic interactions mediated by alkyl side chains in a homologous series of amino acids. The ω-amine functions of diaminopropionic acid (DAPA), diaminobutyric acid (DABA), ornithine, and lysine were covalently labeled with a luminescent $[Ru(bipy)_3]^{2+}$ fragment. Protonation of the α-amine function results in a significant dependence of nonradiative excited-state decay rates on the number of methylene groups, *n*, in the respective side chain. Two analogous series of compounds in which the α-amino acid moiety was replaced by $R–NH_2$ or $R–NMe_3^+$ have been studied for comparison. It was found that the emission energies of the chromophore and the pK_A values of the remote amine functional groups in our complexes are both affected by inductive effects which can be described by a Hammett–Taft type relationship. We were able to show that the induction decays with $1/n$, where n = the number of methylene groups separating the chromophore from the amine and ammonium functions. A qualitative description of the phenomenon is given in terms of acid base theory.

Introduction

Peptides and peptide analogues are among the most versatile components for the biomimetic development of new compounds and materials. Examples include pharmaceuticals,[1] enzyme mimetics,[2–4] building blocks for combinatorial catalyst screenings,[5–7] light-harvesting peptides[8,9] and model compounds for electron-transfer proteins.[10–13] The unsurpassed adaptability of peptide scaffolds is achieved by a surprisingly simple building-block design. It remains a fascinating practical and intellectual challenge for chemists to study and understand the subtle interactions between individual amino acid functions which as a whole determine the function of the assembly.

The basic starting point for investigations of electronic interactions between side-chain functional groups and their microenvironment is amino acids and small peptides. Absorption[14,15] and resonance Raman spectra[16] and the characterization of photodegradation products[17] provide evidence for charge transfer processes involving the amide backbone and aromatic side chains. These processes can be modulated by inductive effects imposed by additional functional groups. An *N*-terminal ammonium ion has been shown to induce higher rates of photoinduced electron transfer reactions in phenylalanine containing peptides.[18]

A related effect is also responsible for the unusual photophysical properties of the ruthenium-substituted amino acids **1a–4a** shown in Figure 1. We have recently shown[19] that the ruthenium-based emission is quenched by protonation of the remote amino acid NH_2 group. Nonradiative decay rates increase as the number of methylene groups, *n*, decreases. Questions concerning the origin of this be-

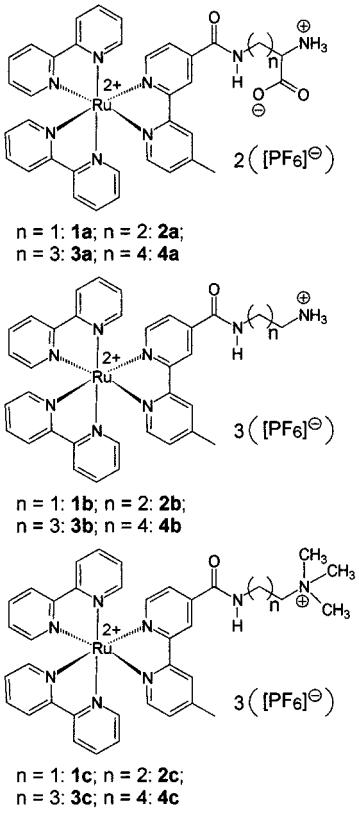

Figure 1. Structures of all compounds investigated in this work

[a] Institute of Inorganic Chemistry, University of Erlangen, Egerlandstraße 1, 91058 Erlangen, Germany
Fax: (internat.) + 49–9131/852–7387
E-mail: Alsfasser@chemie.uni-erlangen.de
[b] Institute of Physical Chemistry, University of Erlangen, Egerlandstraße 3, 91058 Erlangen, Germany
[c] Institute of Molecular Chemistry, University of Amsterdam, Nieuwe Achtergracht 166, 1018 WV Amsterdam, The Netherlands

  1434–1948/01/0202–0439 $ 17.50+.50/0

havior have prompted us to study the amine and tetraalkylammonium derivatives **1b−4b** and **1c−4c**, respectively (Figure 1). Our results now enable us to propose a model which explains our observations.

The inductive effect of an ammonium functional group is interpreted in terms of acid-base interactions as defined by the ECT concept developed by Drago et al.[20,21] A semiquantitative analysis is possible by the introduction of a distance dependent Hammett−Taft σ-parameter.[22,23] This conceptual framework may contribute to a better understanding of inductive effects and serve as a starting point for more detailed quantitative analyses of electronic interactions in peptides and proteins.

Results

Synthesis and Characterization

The amine derivatives **1b−4b** were prepared analogously to the amino acids **1a−4a** starting from the succinimide ester $[Ru(bipy)_2(m\text{-OSu})](PF_6)_2$ [9] and the respective mono-*t*Boc protected diamine. Reaction of **1b−4b** with an excess of methyl iodide afforded the trimethylammonium complexes **1c−4c**. All compounds were purified by ion-exchange column chromatography and isolated as hexafluorophosphate salts. The products were characterized and their purity checked by ^{1}H NMR spectroscopy, FAB-MS, and C,H,N-elemental analysis.

NMR Titrations

Ground state pK_A values of the amine groups in **1b−4b** were determined by the same method as described recently for the amino acid complexes **1a−4a**.[19] The respective α-CH resonances were plotted as a function of pH (D_2O) and the curves were fit to a two-state acid base equilibrium.[24,25] Table 1 summarizes the pK_A values determined for the amine functions of our complexes together with some literature data.

Table 1. pK_A(NH_2/NH_3^+) values of **1a−4a**[19] and **1b−4b** as determined by NMR- (pK_A) and luminescence spectroscopy (pK_A*), respectively

Compound	pK_A	pK_A*
1a	8.59 ± 0.02	8.82 ± 0.05
2a	9.33 ± 0.02	9.37 ± 0.09
3a	9.64 ± 0.02	10.21 ± 0.19
4a	9.80 ± 0.03	10.10 ± 0.51
1b	9.21 ± 0.01	9.27 ± 0.04
2b	10.23 ± 0.03	10.18 ± 0.07
3b	10.75 ± 0.01	10.80 ± 0.16
4b	11.22 ± 0.02	10.37 ± 0.37
DAPA[26]	6.68	
DABA[26]	8.19	
Orn[26]	8.78	
Lys[26]	9.12	
Ethylenediamine[27]	10.71/7.56	
Propylenediamine[27]	10.94/9.03	
Butylenediamine[27]	11.15/9.71	
Asn[26]	8.72	
Gln[26]	9.01	

The pK_A values of the respective amine functions in **1a−4a** and **1b−4b** are strongly affected by the presence of the ruthenium chromophore. The α-NH_3^+ groups of our ruthenium-substituted amino acids are considerably less acidic than those of the respective parent compounds diaminopropionic acid (DAPA), diaminobutyric acid (DABA), ornithine, and lysine.[26] Similarly, the pK_A values of the ammonium groups in **1b−4b** are higher than those reported for the second protonation of the respective diamine.[27] It is interesting to note that the pK_A values obtained for **1a** and **2a** compare well with those reported for the two ω-amido-α-amino acids asparagine and glutamine. This suggests that the amino acid groups are more strongly affected by the amide function than by the ruthenium complex fragment.

Absorption and Resonance Raman Spectra

The UV/Visible spectra of the twelve complexes **1(a-c)−4(a-c)** are indistinguishable within experimental error and are typical for polypyridyl ruthenium complexes. No significant spectral changes are observable at pH values ranging from 0 to 14. A characteristic broad band at 457 nm with a shoulder at 430 nm is assigned to the MLCT transitions involving the unsubstituted and amide-substituted bipyridine ligands.

Resonance Raman spectra for **1a** were collected in order to evaluate further the contributions of the different bipyridine ligands to the absorption bands. Excitation wavelengths (λ_{exc}) of 433, 457.9, and 488 nm, respectively, were used which cover the MLCT band of the complex. Measurements at three different pH values (1, 7, and 12) show that the spectra do not vary significantly with pH.

The strongest bands are summarized in Table 2. They are found above 1000 cm^{-1} and belong to stretching vibrations of the ligands. No vibration of the amino acid moiety is resonance enhanced. The relative signal intensities significantly depend on the excitation wavelength. A comparison with $[Ru(bipy)_3]^{2+}$ shows that bands at 1608, 1563, 1320, and 1176 cm^{-1} can be assigned to vibrations involving the unsubstituted bipyridine rings in **1a**. They are strongest at λ_{exc} = 433 nm indicating that the shoulder at the high-energy end of the MLCT band is due to a Ru → bipy charge transfer. Transitions involving the amide-substituted ligand occur at lower energy, which is evident from the Raman bands at 1622, 1547, 1277, and 1214 cm^{-1} which increase as λ_{exc} is raised to 488 nm. Finally, the strongest Raman band is located at 1491 cm^{-1} and reveals a shoulder at its low-energy end (ca. 1483 cm^{-1}) when λ_{exc} = 488 nm.

Table 2. Selected resonance Raman bands ($\tilde{\nu}$, cm^{-1}) assignable to the unsubstituted (bipy) and amino acid substituted (bipy−AA) bipyridine ligands of **1a**

Ligand	1. Set	2. Set	3. Set	4. Set	5. Set
bipy	1608	1563	1491	1320	1176
bipy−AA	1622	1547	1483 (sh)	1277	1214

Table 3. Cyclic voltammetry data for **1a−4a**, **1b−4b**, and **1c−4c**

Compd.	$Ru^{II/III}$ obsd. $E_{1/2}$, V (ΔEp, mV)	Ligand reductions obsd. $E_{1/2}$, V (ΔEp, mV)		
1a	1.33 (80)	−1.30 (70)	−1.49 (70)	−1.72 (70)
2a	1.33 (90)	−1.31 (70)	−1.54 (60)	−1.73 (80)
3a	1.32 (100)	−1.30 (60)	−1.54 (50)	−1.75 (90)
4a	1.32 (90)	−1.31 (60)	−1.51 (130)	−1.72 (110)
1b	1.33 (90)	−1.27 (70)	−1.47 (70)	−1.71 (110)
2b	1.33 (90)	−1.22 (80)	−1.46 (90)	−1.70 (90)
3b	1.32 (80)	−1.22 (80)	−1.46 (70)	−1.70 (80)
4b	1.32 (90)	−1.23 (70)	−1.46 (80)	−1.70 (80)
1c	1.31 (100)	−1.33 (80)	−1.54 (80)	−1.83 (110)
2c	1.32 (90)	−1.34 (80)	−1.54 (80)	−1.83 (110)
3c	1.32 (90)	−1.34 (80)	−1.54 (80)	−1.77 (100)
4c	1.32 (90)	−1.34 (80)	−1.53 (90)	−1.73 (90)

Our data compare well with time-resolved resonance Raman studies reported by Meyer et al[28] for the lysine derivative **4a** in acetonitrile. The assignment of the low-energy transitions to charge-transfer processes involving the amide-substituted pyridine ring is consistent with a lower reduction potential of this ligand. It is important for the arguments presented in the following discussion that the MLCT transition involving the amino acid ligand bpy-DAPA is largely obscured by transitions to the unsubstituted bipyridines. This prevents an accurate determination of λ_{max} for the Ru → bpy-DAPA transition.

Cyclic Voltammetry

The cyclic voltammogram of each complex in acetonitrile is characterized by four reversible waves. Table 3 summarizes these data. Oxidation of the respective ruthenium(II) center is observed at a potential of ca. +1.32 V (vs. Ag/AgCl). The first ligand reduction occurs at a potential of ca. −1.3 V. Consistent with literature data of related complexes,[29] and our resonance Raman studies, we assign this wave to the reduction to the amide-substituted pyridine ring.

Whereas the oxidation waves are clearly independent of the bipyridine substituents, small differences are observed for the ligand reduction potentials. The amine complexes **1b−4b** appear to be more easily reducible than their amino acid and tetraalkylammonium analogues **1a,c-4a,c**. However, considering the broad waves which are typical for the class of complexes investigated this difference may not be significant.

Emission Spectra

The emission spectra of **1a−4a** and **1b−4b** are strongly pH dependent. In Figure 2, the uncorrected maximum emission intensities are plotted as a function of pH. Two protonation steps are clearly separated in each case. The inflection point at ca. pH 0.5 is assigned to protonation of the amide link.[19] The second inflection is due to protonation/deprotonation of the respective amine functions. The magnitude of the observed change in luminescence intensity depends on the number of methylene spacers separating the amide link from the α-C atom. The spectra of the amino acids and the ethylenediamine derivatives show very similar pH dependences except for a significant difference in the observed pK_A values. All luminescence titration curves yield pK_A values for the amine groups which are very similar to those obtained by NMR spectroscopy, suggesting similar acid-base properties of the ground and excited states. The results obtained from emission spectroscopy are also summarized in Table 1.

Lifetime measurements performed for all complexes at pH 0, 4.8, and 12 confirm our findings from steady state measurements. We have repeated and reproduced all lifetime experiments reported earlier[19] in order to assure that all data were obtained under the same conditions. These results are presented in Table 4. Amide protonation at low pH values results in large nonradiative decay rates (τ = ca. 60 ns) for all compounds. In the pH range between the two inflections shown in Figure 2, lifetimes increase with the number of methylene spacers, *n*. The values obtained for **1a** (τ = 345 ns) and **1b** (τ = 355 ns) at pH 4.8 compare well. At pH 12 we find very similar values of ca. 420 ns for all four amino acids. In the case of the amine derivatives **1b−4b** this number is slightly smaller (396 ns). We think that this difference is significant and may be due to medium effects associated with the high base concentration. As will be shown in the Discussion section, high pH values also

Table 4. pH-Dependent luminescence lifetimes τ (ns) of **1a−4a**, **1b−4b**, and **1c−4c**

Compd.	pH 0	pH 4.8	pH 12
1a	64 ± 1	345 ± 8	427 ± 2
2a	77 ± 1	389 ± 5	427 ± 2
3a	61 ± 1	428 ± 7	420 ± 3
4a	59 ± 1	430 ± 1	413 ± 1
1b	53 ± 1	355 ± 1	396 ± 3
2b	54 ± 1	389 ± 2	402 ± 2
3b	50 ± 1	404 ± 2	405 ± 2
4b	50 ± 1	407 ± 1	404 ± 2
1c	61 ± 1	352 ± 4	345 ± 3
2c	53 ± 2	399 ± 3	393 ± 1
3c	52 ± 1	423 ± 2	412 ± 1
4c	50 ± 1	422 ± 1	412 ± 2

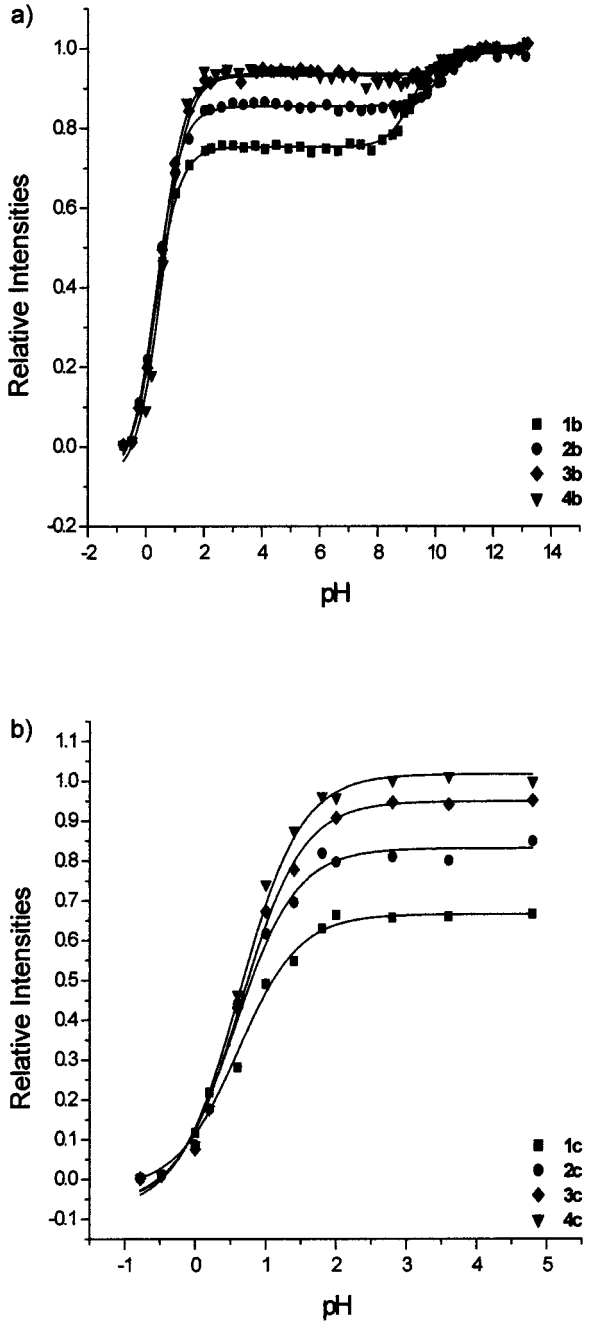

Figure 2. Luminescence intensities of (a) **1b−4b** and (b) **1c−4c** as a function of pH; intensities of **1b−4b** are relative to the values of the respective compound at pH 12, intensities of **1c−4c** are relative to the value of **4c** at pH 4.8

affect the lifetimes of the trimethylammonium complexes **1c−4c**.

The trimethylammonium complexes **1c−4c** were prepared in order to evaluate possible contributions of NH bonds to nonradiative decay processes.[30] The compounds exhibit lifetimes of 352 ns (**1c**), 399 ns (**2c**), 423 ns (**3c**), and 422 ns (**4 c**) at pH 4.8. These numbers also compare well with the data obtained for our series of amino acids, indicating that NH bonds are not involved in energy dissipation pathways. Slightly smaller values are observed at pH 12, indicating a small contribution of the basic medium to excited-state decay processes. In summary, our results demonstrate that a zwitterionic amino acid function, an ammonium ion, and a tetraalkylammonium ion have the same effects on the excited state properties of a $[Ru(bipy)_3]^{2+}$ chromophore.

Discussion

Our data demonstrate that the luminescence properties of the $[Ru(bipy)_3]^{2+}$ chromophores in **1(a-c)−4(a-c)** are affected by protonation of the amide link at very low pH, as well as by the presence of NR_4^+ functions in (i) the zwitterionic amino acid groups of **1a−4a**, (ii) the ammonium ions in **1b−4b**, and (iii) the trimethylalkylammonium groups in **1c−4c**. Two conclusions can be drawn from a comparison of the three series of compounds investigated: (i) the reduced lifetimes of the compounds with short alkyl spacers originate from the intramolecular presence of an NR_4^+ function and do not require a zwitterionic amino acid structure, and (ii) a direct participation of NH units in energy dissipation pathways is ruled out since the $RNMe_3^+$ compounds **1c−4c** do not differ significantly from the RNH_3^+ derivatives **1a,b−4a,b**. The latter conclusion is particularly important since hydrogen bonding to the solvent[31] and high energy NH vibrations are known to significantly effect nonradiative decay rates in other systems.[30]

It is evident from the emission spectra shown in Figure 3 that decreasing intensities are associated with a small but significant band-shift to lower energies. This observation suggests that the energy gap between the excited state and the ground state is affected. A contribution to the nonradiative decay rate constants according to the energy gap law is therefore evident. However, the differences between the emission maxima are very small making a quantitative analysis difficult. Figure 4 contains a plot of ln*k* versus emission energies which includes literature data reported for $[Ru(bipy)_3]^{2+}$.[32] The comparison in Figure 4b clearly shows that, in fact, the very small shift in energies observed for our compounds is sufficient to account for the observed differences in nonradiative decay rates. It should be noted that $[Ru(bipy)_3]^{2+}$ cannot be included without caution since linear energy-gap relationships are only expected within a series of closely related complexes. In addition, it has been reported that solvent effects in hydroxylic solutions may result in significant deviations from a simple linear energy-gap dependence.[33,34] As is shown in Figure 4b the linear fit obtained for our complexes alone is slightly steeper than that obtained if $[Ru(bipy)_3]^{2+}$ is included. However, we think the data show that the structure and pH-dependent nonradiative decay rates of our complexes can conveniently be explained in terms of the energy-gap law. This is important since we do not have any evidence for other well-known effects such as the participation of low lying d-d excited states,[35] solvent reorganization,[36] or different geometric displacements in the excited state.[37,38] These phenomena should manifest themselves in ligand loss or emission band shapes.

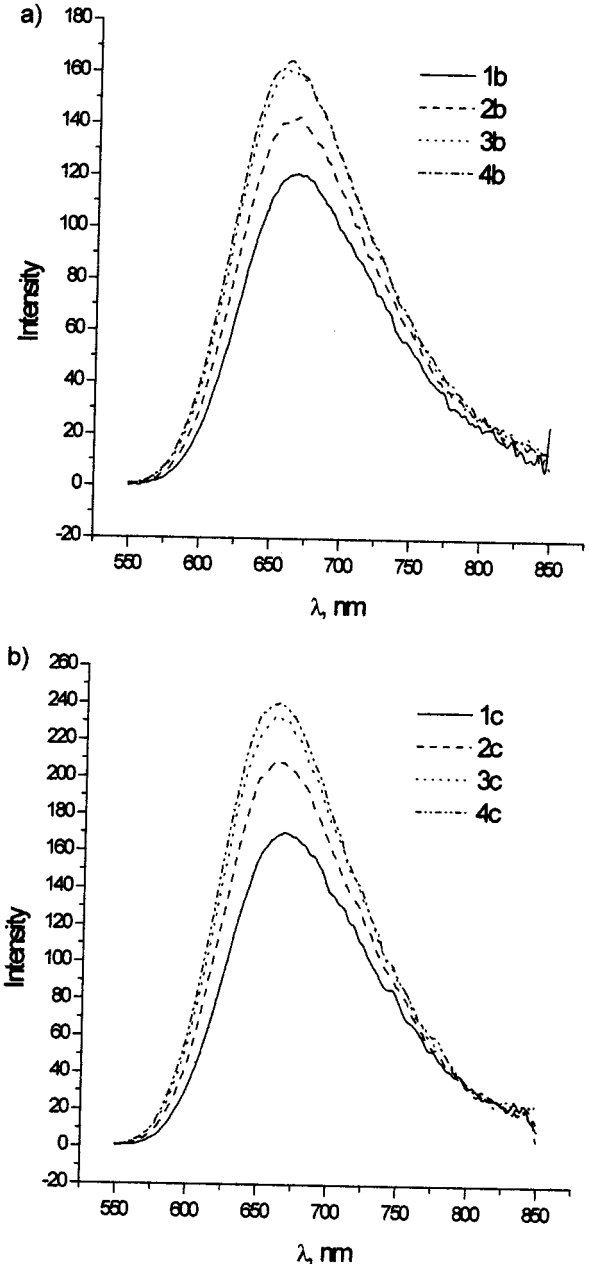

Figure 3. Corrected luminescence spectra measured at pH 4.8: a) **1b−4b**, b) **1c−4c**

The origin of the decreasing emission energies is most likely an inductive effect caused by the ammonium groups in our complexes. An electronic interaction between the ruthenium chromophore and the remote amine functions is evident from the ground state pK_A values given in Table 1. The NH_3^+ groups in **1a−4a** and **1b−4b** become more acidic as the number of methylene groups decreases. Similarly, the electron affinity of the ruthenium chromophore must increase in the presence of an ammonium group. This results in a lower HOMO−LUMO energy gap and explains our observations. A similar effect has been described by Seidel et al., who reported the influence of *N*-terminal ammonium groups on photoinduced electron transfer rates in tyrosine peptides.[18]

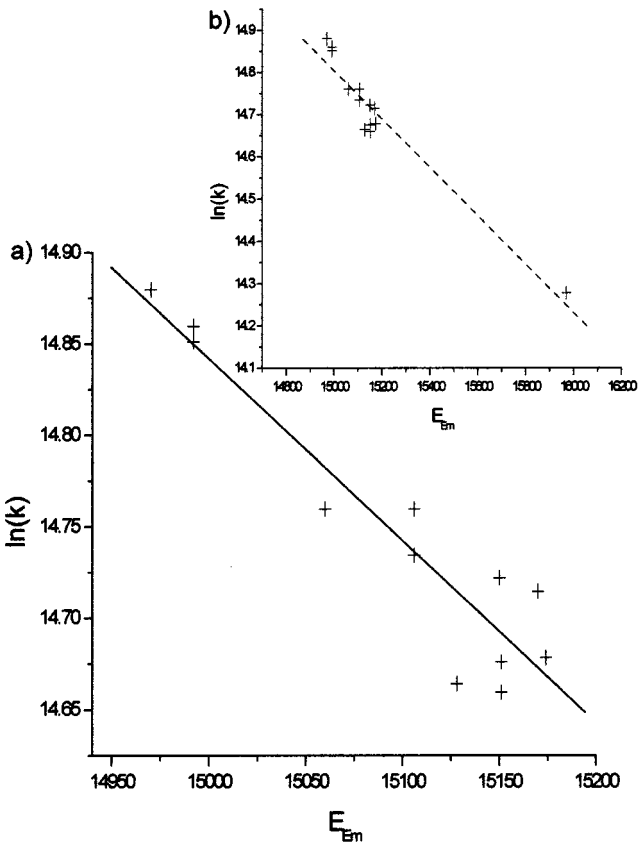

Figure 4. (a) Plot of ln k vs. E_{em} (pH = 4.8) for all compounds reported in this work; (b) comparison with the literature value reported for $[Ru(bipy)_3]^{2+}$ (see ref. [49])

Further support for an explanation which only involves an energy gap law relationship comes from the behavior of our complexes at low pH values. We have shown in a previous article[19] that protonation of the amide oxygen atom in **1a−4a** is associated with a large red shift of the emission energies. Resonance structures of the excited state can be drawn with the negative charge localized at the amide functional group and it is evident that protonation of this group will result in a lower reduction potential of the substituted bipyridine ligand.

We suggest that a qualitative description of the observed phenomena can be given in terms of acid-base interactions between the Lewis acid NR_4^+ and the Lewis basic amide link. Drago et al.[20,21] have developed the ECT-concept which splits acid-base interactions into three contributions. The first one, $C_{acid}C_{Base}$, describes covalent interactions and is irrelevant here since acid and base are separated by an alkyl chain in our complexes. The second one, $E_{Acid}E_{Base}$, originates in electrostatic interactions and may be the most important in determining the pK_A(NH_2/NH_3^+) values in **1b−4b**. The third contribution, $R_{Acid}T_{Base}$, (R: Receptance, T: Transmission) refers to an exchange of electron density between the acid and the base. The ECT parameters are closely related to the physical parameters electron affinity (EA), ionization energy (IE), and electronegativity as defined by the Jaffé scale.[39−41] Consideration of the electron transfer interaction $R_{Acid}T_{Base}$ may explain why a zwitter-

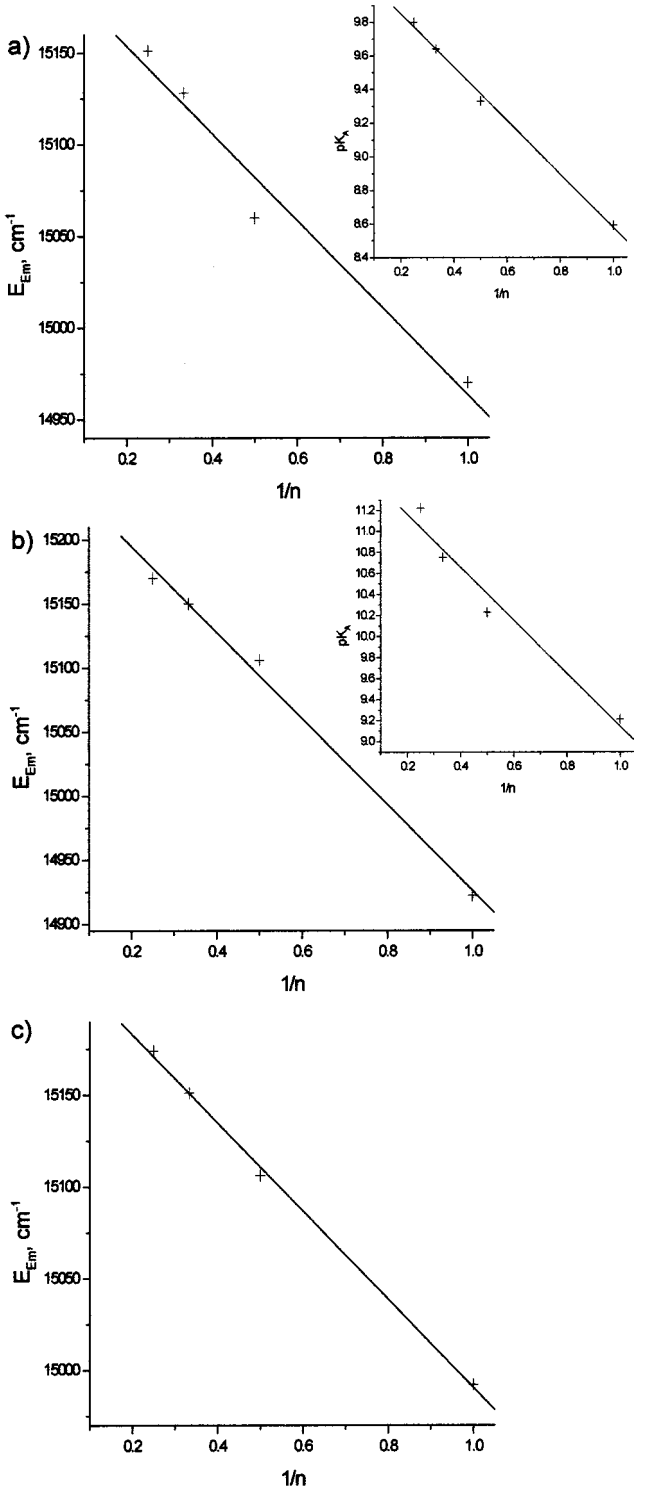

Figure 5. Plots of pK_A values (NH_2/NH_3^+) and emission energies (pH 4.8), respectively, vs. 1/*n*: (a) **1a−4a**, (b) **1b−4b**; (c) plot of the emission energies of **1c−4c** at pH 4.8 vs. 1/*n*

ionic amino acid (0 charge) and an ammonium function (+1 charge) can have the same effect on the LUMO energy of a conjugated chromophore.

The significant changes in pK_A(NH_2/NH_3^+) values observed for our amino acid (**1a−4a**) and amine (**1b−4b**) complexes indicate that inductive effects have to be relevant not only in the excited states, but also in the ground states of the molecules. It must therefore be explained why the decreased HOMO−LUMO gap is not manifest in changes of the absorption spectra and reduction potentials. The differences in emission energies, ΔE_{em}, are on the order of 2 kJ/mol between the two extremes within each series (**1a/4a**, **1b/4b**, **1c/4c**). This would correspond to an estimated change in redox potentials of ca. 20 mV, a value which is not significant within the experimental error of our cyclic voltammograms. As has been discussed above, the same is true for the absorption spectra of our complexes, which are largely obscured by overlapping MLCT bands. The resonance Raman spectra show that the MLCT transition to the substituted bipy ligand is covered by the Ru → bipy transition, which is more intense due to the presence of two unsubstituted bipyridine ligands. This makes a determination of the absorption energy corresponding to the Ru → substituted bipy transition impossible. It is evident that effects which are readily observable by emission spectroscopy cannot be determined by either absorption spectroscopy or cyclic voltammetry.

Inductive effects are usually described semi-quantitatively by linear free-energy relationships such as the Hammett[22] and Taft[23] equations. In a correlation analysis, rate constants or physical properties such as chemical shifts or IR frequencies[42] are plotted as a function of a parameter, σ, which is a measure of the magnitude of the electron-donating or -withdrawing effect imposed by a functional group. In our study the functional groups do not vary and the inductive effect is only a function of the number of methylene groups separating the chromophore from the ammonium function. As is shown in Figure 5, both pK_A values and emission energies give reasonably good straight lines when they are plotted against 1/*n*, where *n* is the number of methylene spacers as defined by Figure 1. Consequently, ln*k* also shows a linear dependence on 1/*n* and pK_A, respectively. This is shown in Figure 6. Thus, 1/*n* describes the decrease of σ with increasing alkyl chains separating a Lewis acid from a Lewis base. This relationship holds for zwitterionic amino acids as well as for ammonium ions and should therefore be a measure of similar effects in a large variety of different compounds including peptides and proteins.

Though four data points are a small basis for a quantitative correlation all the series behave similarly, thus supporting our interpretation. An interesting aspect is revealed by the ln*k* vs. 1/*n* plots obtained for the trimethylammonium complexes **1c−4c** at pH 4.8 and pH 12. The two lines are parallel with slightly higher nonradiative decay rates observed at high base concentration. This observation can be assigned to a medium effect which is comparable to the small ionic-strength contributions observed for nonradiative decay rates of the $[Ru(bipy)_3]^{2+}$ excited state.[43]

A few problems should finally be noted. Due to their inherent flexibility, alkyl chains prevent a quantitative analysis of distance effects between two functional groups. The number of bonds or the number of methylene groups, *n*, has to be used instead. In addition, the amide link applied in our study may result in the formation of *syn* and *anti*

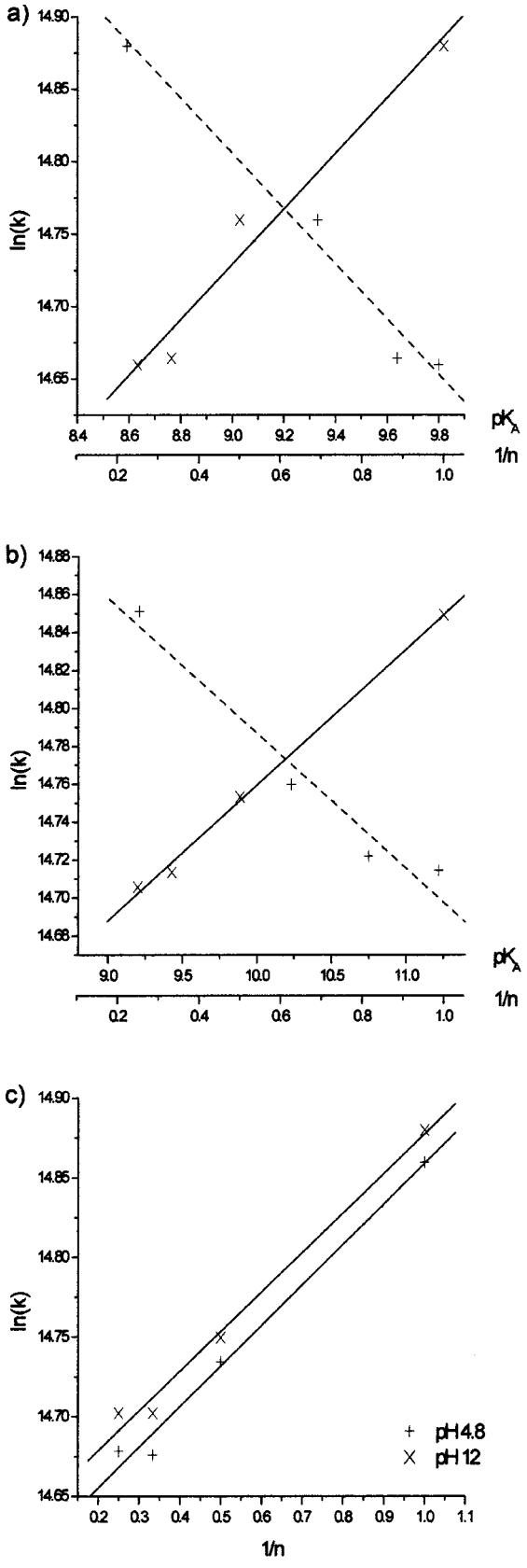

Figure 6. Plots of ln k vs. 1/n (solid lines, x) and pK_A values (dashed lines, +), respectively: (a) **1a−4a**, (b) **1b−4b**; (c) Plot of ln k vs. 1/n for **1c−4c** at pH 4.8 and pH 12, respectively

isomers which is a known complication in the quantitative analysis of photoinduced electron-transfer reactions involving amide-bridged donor-acceptor dyads.[44] Furthermore, alkyl bridges are known to effect electrostatic interactions since they modify the microscopic dielectric constant between the two relevant functional groups.[45] As a consequence, our empirical correlations are not suitable for a quantitative evaluation of different contributions such as the magnitude of electrostatic ($E_{Acid}E_{Base}$) or electron transfer ($R_{Acid}T_{Base}$) interactions. Detailed theoretical studies will be required to tackle these problems. However, with our proposed model we provide a starting point for such investigations.

Conclusions

Our studies concerning the photophysical properties of chromophore-substituted amino acids have lead us to propose a model for the interpretation of inductive effects in amino acids and peptides. Two observations are particularly important:
(1) The pK_A value of a remote functional group and the HOMO−LUMO gap of a chromophore are linearly related. This may be relevant for the interpretation of pH titration curves particularly in small molecular assemblies were meaningful assignments of pK_A values can be made.
(2) 1/n can be used to describe the decay of the electronic Hammett−Taft parameter, σ, when an increasing alkyl bridge separates two functional groups. Our data show that σ/n is significant in **1a** but very small in the lysine derivative **4a**. This may help to define the limiting case for "through-bond" interactions mediated by amino acid side chains in small peptide assemblies[13,28,29,46] and proteins.[47]

Experimental Section

Materials: $[Ru(bipy)_2Cl_2]$[48], $[Ru(bipy)_2(m\text{-OH})](PF_6)_2$ [9] and $[Ru(bipy)_2(m\text{-OSu})](PF_6)_2$ (m = 4-carbonyl-4′-methyl-2,2′-bipyridine, m-OSu = 4-carboxysuccinimidoester-4′-methyl-2,2′-bipyridine) were prepared according to the method reported by Erickson et al.[9] $RuCl_3$ was a donation from Degussa. Reagent grade solvents were obtained from Roth, NMR solvents from Aldrich and all other chemicals from Fluka. Water for preparations was demineralized. All reactions were carried out under argon.

Spectra were recorded with the following instruments: UV/Vis: Shimadzu UV-2101PC. − IR (KBr pellets): Mattson Polaris FT IR. − ^{1}H NMR: Bruker Avance DPX 300. All chemical shifts are referenced to residual solvent signals as internal standards previously referenced to TMS, with high-frequency shifts recorded as positive. Pyridine resonances are labelled "b" for the bipy, and "m" for the substituted bipy ligands, respectively. − Elemental analysis: Carlo Erba EA 1106. − FAB: Micromass ZabSpec mass spectrometer.

$[Ru(bipy)_2\{m\text{-}CONH(CH_2)_nNH_3^+\}](PF_6)_3$ (n = 2: 1b, 3: 2b, 4: 3b, 5: 4b). − General Procedure: $[Ru(bipy)_2(m\text{-OH})](PF_6)_2$ and HOSu (1.1 equiv.) were dissolved in acetonitrile (5 mL) and the solution was cooled to 0 °C. Dicyclohexylcarbodiimide (DCC, 2.5 equiv.) was added and the red suspension was stirred at 0 °C for 5 h. The

precipitated urea was filtered off and washed several times with small amounts of acetonitrile. The *N*-Boc-monoprotected diamine (1.2 equiv.) was added to the filtrate and the reaction mixture was stirred for 1.5 h at 41 °C. After removal of all the acetonitrile by rotary evaporation, the residue was suspended in a mixture of dioxane (20 mL) and 4 N HCl (6 mL) and stirred for 1 h at 0 °C. All solvent was removed by rotary evaporation and the residue dried under vacuum. The obtained solid was dissolved in water (100 mL), neutralized with 2 M NaOH and purified by ion exchange chromatography (Sephadex CM-50) with an NaCl gradient in aqueous phosphate buffer (0.6 mM, pH = 7.2). A first band was obtained at 10 mM NaCl which contained traces of $[Ru(bipy)_2(m\text{-}OH)]^{2+}$. The product was eluted with 80 mM NaCl. Rotary evaporation to dryness afforded an orange solid which was suspended in a minimum volume of methanol. The suspension was filtered to remove insoluble salts, all methanol stripped by rotary evaporation and the resulting red solid dried in vacuo.

The crude products were dissolved in water (20 mL), precipitated with a 1.5-fold excess of NH_4PF_6 in water (1 mL) and stirred for 1 h at room temp. HPF_6 (60%, 1.5 equiv.) was added to yield the compounds in their fully protonated form. After 10 min. the brown-orange precipitate was isolated by filtration, washed with cold 0.1 M HPF_6 (3 × 5 mL) and dried in a vacuum desiccator over silica gel.

1b: Yield: 890 mg (74%). − ^{1}H NMR (300 MHz, CD_3OD): δ = 2.58 (s, 3 H, m4′-CH_3), 3.22 (t, 2 H, $CH_2CH_2NH_3^+$), 3.73 (t, 2 H, $CH_2CH_2NH_3^+$), 7.34 (d, 1 H, m5′), 7.47 (m, 4 H, b5), 7.62 (d, 1 H, m5), 7.79 (m, 5 H, 4 × b6, m6′), 7.94 (d, 1 H, m6), 8.09 (m, 4 H, b4), 8.64 (m, 5 H, 4 ×b3, m3′), 8.95 (s, 1 H, m3). − IR (KBr pellets, cm^{-1}): $\tilde{\nu}$ = 3080 (m), 2926 (m), 1657 (m), 1543 (m), 1466 (m), 1449 (m), 1311 (m), 842 (vs, PF_6^-), 765 (s), 559 (s). − UV/Vis (H_2O): λ_{max} (lg ε, M^{-1} cm^{-1}) = 456 (4.24), 288 (4.95), 245 nm (4.44). − FAB$^+$ (*m*-NBA): *m*/*z* = 961 [$M^+ - PF_6^-$], 815 [$M^+ - 2\ PF_6^-$]. − $C_{34}H_{33}F_{18}N_8OP_3Ru{\cdot}H_2O$ (1105.6 + 18): calcd. C 36.34, H 3.14, N 9.97; found C 36.44, H 3.10, N 9.66.

2b: Yield: 951 mg (78%). − ^{1}H NMR (300 MHz, CD_3OD): δ = 1.96 (q, 2 H, $CH_2CH_2CH_2NH_3^+$), 2.59 (s, 3 H, m4′-CH_3), 3.04 [t, 2 H, $(CH_2)_2CH_2NH_3^+$], 3.55 [t, 2 H, $CH_2(CH_2)_2NH_3^+$], 7.34 (d, 1 H, m5′), 7.47 (m, 4 H, b5), 7.61 (d, 1 H, m5), 7.80 (m, 5 H, 4 × b6, m6′), 7.91 (d, 1 H, m6), 8.09 (m, 4 H, b4), 8.64 (m, 5 H, 4 ×b3, m3′), 8.96 (s, 1 H, m3). − IR (KBr pellets, cm^{-1}): $\tilde{\nu}$ = 3114 (m), 3083 (m), 2934 (m), 1630 (m), 1544 (m), 1465 (m), 1447 (m), 1261 (m), 1163 (m), 845 (vs, PF_6^-), 766 (s), 559 (s). − UV/Vis (H_2O): λ_{max} (lg ε, M^{-1} cm^{-1}) = 456 (4.24), 288 (4.95), 245 nm (4.45). − FAB$^+$ (*m*-NBA): *m*/*z* = 975 [$M^+ - PF_6^-$], 830 [$M^+ - 2\ PF_6^-$]. − $C_{35}H_{35}F_{18}N_8OP_3Ru{\cdot}H_2O$ (1119.7 + 18): calcd. C 36.95, H 3.28, N 9.85; found C 36.64, H 3.34, N 9.36.

3b: Yield: 890 mg (72%). − ^{1}H NMR (300 MHz, CD_3OD): δ = 1.74 (m, 4 H, -$CH_2CH_2CH_2CH_2NH_3^+$), 2.59 (s, 3 H, m4′-CH_3), 2.98 [m, 2 H, $(CH_2)_3CH_2NH_3^+$], 3.49 [m, 2 H, $CH_2(CH_2)_3NH_3^+$], 7.34 (d, 1 H, m5′), 7.47 (m, 4 H, b5), 7.61 (d, 1 H, m5), 7.78 (m, 5 H, 4 × b6, m6′), 7.91 (d, 1 H, m6), 8.10 (m, 4 H, b4), 8.65 (m, 5 H, 4 ×b3, m3′), 8.96 (s, 1 H, m3). − IR (KBr pellets, cm^{-1}): $\tilde{\nu}$ = 3117 (m), 3083 (m), 2939 (m), 1652 (m), 1543 (m), 1466 (m), 1448 (m), 1239 (m), 1163 (m), 843 (vs, PF_6^-), 765 (s), 559 (s). − UV/Vis (H_2O): λ_{max} (lg ε, M^{-1} cm^{-1}) = 456 (4.22), 287 (4.94), 246 nm (4.44). − FAB$^+$ (*m*-NBA): *m*/*z* = 989 [$M^+ - PF_6^-$], 843 [$M^+ - 2\ PF_6^-$]. − $C_{36}H_{37}F_{18}N_8OP_3Ru{\cdot}3H_2O$ (1133.7 + 54): calcd. C 36.40, H 3.64, N 9.43; found C 35.93, H 3.29, N 9.66.

4b: Yield: 750 mg (75%). − ^{1}H NMR (300 MHz, CD_3OD): δ = 1.47 [m, 2 H, $(CH_2)_3CH_2CH_2NH_3^+$], 1.69 [m, 4 H, $CH_2CH_2CH_2(CH_2)_2NH_3^+$], 2.58 (s, 3 H, m4′-$CH_3$), 2.95 [t, 2 H, $(CH_2)_4CH_2NH_3^+$], 3.46 [t, 2 H, $CH_2(CH_2)_4NH_3^+$], 7.33 (d, 1 H, m5′), 7.46 (m, 4 H, b5), 7.61 (d, 1 H, m5), 7.79 (m, 5 H, 4 × b6, m6′), 7.91 (d, 1 H, m6), 8.09 (m, 4 H, b4), 8.64 (m, 5 H, 4 ×b3, m3′), 8.95 (s, 1 H, m3). − IR (KBr pellets, cm^{-1}): $\tilde{\nu}$ = 3078 (m), 2933 (m), 1652 (m), 1544 (m), 1465 (m), 1444 (m), 1240 (m), 1139 (m), 844 (vs, PF_6^-), 764 (s), 559 (s). − UV/Vis (H_2O): λ_{max} (lg ε, M^{-1} cm^{-1}) = 455 (4.24), 286 (4.95), 246 nm (4.44). − FAB$^+$ (*m*-NBA): *m*/*z* = 1003 [$M^+ - PF_6^-$], 858 [$M^+ - 2\ PF_6^-$]. − $C_{37}H_{39}F_{18}N_8OP_3Ru{\cdot}2H_2O$ (1147.7 + 36): calcd. C 37.54, H 3.66, N 9.47; found C 37.23, H 3.78, N 9.34.

[Ru(bipy)$_2${*m*-CONH(CH$_2$)$_n$N(CH$_3$)$_3^+$}](PF$_6$)$_3$ (*n* = 2: 1c, 3: 2c, 4: 3c, 5: 4c). − General Procedure: $[Ru(bipy)_2\{m\text{-}CONH(CH_2)_n\text{-}NH_3^+\}](PF_6)_3$ (**1b−4b**; 0.27 mmol), sodium carbonate (5.1 mmol, 540 mg) and sodium iodide (0.14 mmol, 20 mg) were suspended in acetonitrile (20 mL). After 10 min., methyl iodide (0.98 mmol, 61 μL) was added and the red suspension was stirred in the dark for 2 days. Insoluble salts were filtered off, all solvent stripped by rotary evaporation and the resulting red solid dried overnight under vacuum. The complexes were purified by ion-exchange chromatography and isolated as described above for the diamine compounds, except that no HPF_6 was used and the products were washed with cold 10 mM aqueous NH_4PF_6 (3 × 5 mL).

1c: Yield: 228 mg (72%). − ^{1}H NMR (300 MHz, CD_3OD): δ = 2.58 (s, 3 H, m4′-CH_3), 3.21 (s, 9 H, $N(CH_3)_3^+$), 3.61 [t, 2 H, $CH_2CH_2N(CH_3)_3^+$], 3.90 [t, 2 H, $CH_2CH_2N(CH_3)_3^+$], 7.34 (d, 1 H, m5′), 7.46 (m, 4 H, b5), 7.61 (d, 1 H, m5), 7.78 (m, 5 H, 4 × b6, m6′), 7.92 (d, 1 H, m6), 8.09 (m, 4 H, b4), 8.58 (s, 1 H, m3′), 8.65 (d, 4 H, 4 ×b3), 8.92 (s, 1 H, m3). − IR (KBr pellets, cm^{-1}): $\tilde{\nu}$ = 3118 (m), 3087 (m), 1674 (s), 1541 (m), 1470 (m), 1448 (m), 1309 (m), 841 (vs, PF_6^-), 765 (s), 558 (s). − UV/Vis (H_2O): λ_{max} (lg ε, M^{-1} cm^{-1}) = 457 (4.23), 288 (4.95), 245 nm (4.45). − FAB$^+$ (*m*-NBA): *m*/*z* = 1003 [$M^+ - PF_6^-$], 858 [$M^+ - 2\ PF_6^-$]. − $C_{37}H_{39}F_{18}N_8OP_3Ru{\cdot}H_2O$ (1147.7 + 18): calcd. C 38.1, H 3.55, N 9.61; found C 38.35, H 3.49, N 9.54.

2c: Yield: 223 mg (72%). − ^{1}H NMR (300 MHz, CD_3OD): δ = 2.14 [q, 2 H, $CH_2CH_2CH_2N(CH_3)_3^+$], 2.59 (s, 3 H, m4′-CH_3), 3.16 [s, 9 H, $N(CH_3)_3^+$], 3.44 [m, 2 H, $(CH_2)_2CH_2N(CH_3)_3^+$], 3.58 [t, 2 H, $CH_2(CH_2)_2N(CH_3)_3^+$], 7.33 (d, 1 H, m5′), 7.48 (m, 4 H, b5), 7.61 (d, 1 H, m5), 7.77 (m, 4 H, 4 × b6), 7.88 (d, 1 H, m6′), 8.09 (m, 4 H, b4), 8.58 (s, 1 H, m3′), 8.65 (m, 4 H, 4 × b3), 8.95 (s, 1 H, m3). − IR (KBr pellets, cm^{-1}): $\tilde{\nu}$ = 3118 (m), 3088 (m), 2966 (m), 1671 (s), 1541 (m), 1468 (m), 1448 (m), 1309 (m), 840 (vs, PF_6^-), 765 (s), 558 (s). − UV/Vis (H_2O): λ_{max} (ε, M^{-1} cm^{-1}) = 456 (17000), 289 (90000), 244 nm (28500). − FAB$^+$ (*m*-NBA): *m*/*z* = 1162 [M^+], 1017 [$M^+ - PF_6^-$], 871 [$M^+ - 2\ PF_6^-$]. − $C_{38}H_{41}F_{18}N_8OP_3Ru{\cdot}H_2O$ (1161.8 + 18): calcd. C 38.69, H 3.67, N 9.50; found C 38.52, H 3.65, N 9.18.

3c: Yield: 224 mg (70%). − ^{1}H NMR (300 MHz, CD_3OD): δ = 1.71 [q, 2 H, $(CH_2)_2CH_2CH_2N(CH_3)_3^+$], 1.89 [q, 2 H, $CH_2CH_2(CH_2)_2N(CH_3)_3^+$], 2.58 (s, 3 H, m4′-$CH_3$), 3.10 [s, 9 H, $N(CH_3)_3^+$], 3.34 [t, 2 H, $(CH_2)_3CH_2N(CH_3)_3^+$], 3.54 [t, 2 H, $CH_2(CH_2)_3N(CH_3)_3^+$], 7.34 (d, 1 H, m5′), 7.47 (m, 4 H, b5), 7.61 (d, 1 H, m5), 7.79 (m, 4 H, 4 × b6), 7.87 (m, 2 H, m6′, m6), 8.09 (m, 4 H, b4), 8.59 (s, 1 H, m3′), 8.66 (m, 4 H, 4 × b3), 8.94 (s, 1 H, m3). − IR (KBr pellets, cm^{-1}): $\tilde{\nu}$ = 3086 (m), 1736 (m), 1665 (s), 1542 (m), 1468 (m), 1448 (m), 1310 (m), 841 (vs, PF_6^-), 765 (s), 558 (s). − UV/Vis (H_2O): λ_{max} (lg ε, M^{-1} cm^{-1}) = 456 (4.25), 287 (4.95), 245 nm (4.45). − FAB$^+$ (*m*-NBA): *m*/*z* = 1031 [$M^+ - PF_6^-$], 886 [$M^+ - 2\ PF_6^-$]. − $C_{39}H_{43}F_{18}N_8OP_3Ru{\cdot}H_2O$ (1175.8 + 18): calcd. C 39.24, H 3.80, N 9.39; found C 38.91, H 3.75, N 9.00.

4c: Yield: 234 mg (71%). − ^{1}H NMR (300 MHz, CD_3OD): δ = 1.45 [m, 2 H, $(CH_2)_3CH_2CH_2N(CH_3)_3^+$], 1.75 [m, 4 H, $CH_2CH_2CH_2(CH_2)_2N(CH_3)_3^+$], 2.58 (s, 3 H, m4′-$CH_3$), 3.08 [s, 9 H, $N(CH_3)_3^+$], 3.29 [t, 2 H, $(CH_2)_4CH_2N(CH_3)_3^+$], 3.48 [t, 2 H, $CH_2(CH_2)_4N(CH_3)_3^+$], 7.30 (d, 1 H, m5′), 7.46 (m, 4 H, b5), 7.55 (d, 1 H, m5), 7.75 (m, 4 H, 4 × b6), 7.83 (m, 2 H, m6′, m6), 8.07 (m, 4 H, b4), 8.53 (s, 1 H, m3′), 8.59 (d, 4 H, 4 × b3), 8.88 (s, 1 H, m3). − IR (KBr pellets, cm^{-1}): $\tilde{\nu}$ = 3085 (m), 1734 (m), 1667 (s), 1541 (m), 1468 (m), 1448 (m), 1310 (m), 842 (vs, PF_6^-), 765 (s), 558 (s). − UV/Vis (H_2O): λ_{max} (lg ε, M^{-1} cm^{-1}) = 456 (4.27), 288 (4.95), 245 nm (4.44). − FAB$^+$ (*m*-NBA): *m*/*z* = 1045 [M^+ − PF_6^-], 900 [M^+ − 2 PF_6^-]. − $C_{40}H_{45}F_{18}N_8OP_3Ru{\cdot}H_2O$ (1189.8 + 18): calcd. C 39.78, H 3.92, N 9.28; found C 39.86, H 4.30, N 9.06.

Methods: Steady state luminescence spectra were recorded in deoxygenated demineralized water with a Perkin−Elmer LS 50B spectrofluorimeter equipped with a red-sensitive Hamamatsu R928 photomultiplier tube. 10 μM solutions of the complexes at different pH values were used and the emission spectra were corrected for imperfections of the instrument.

The emission and NMR titration curves for $[Ru(bipy)_2\{m\text{-}CONH(CH_2)_nNH_3^+\}](PF_6)_3$ **1b−4b** were obtained as described previously.[19]

Emission lifetimes were measured following excitation of the sample with a laser pulse at 450 nm as delivered by a Nd-YAG laser (B.M. Industries, 5021 DNS/DPS 10, λ = 1064 nm, harmonic generation of 532, 355 and 266 nm, respectively, laser pulse with $\tau_L \approx 6$ ns, beam diameter $d = 7$ mm and maximal repetition rate $f = 10$ Hz, laser pulse energy E_L at the location of the sample ≈ 1 mJ) coupled with an optical parametrical oscillator (OPO, B.M. Industries, OP 901) for generation of the excitation wavelength. Time-resolved detection of the luminescence of the sample after laser excitation was done with a photomultiplier tube in combination with a monochromator (λ_{em} = 630 nm, time resolution 250 ns and 20 ns). The signal of the photomultiplier was read out by a digital storage oscilloscope (DSO, Gould 4072) and transferred to a personal computer for processing, storage and output. All measurements were made with samples previously deoxygenated by purging with nitrogen. The complex concentration was 10 μM in all cases.

Cyclic voltammetry was performed with a PAR potentiostat 263 using a three-electrode cell with glassy carbon working, Ag/AgCl reference and Pt counter electrodes. Deoxygenated acetonitrile solutions of the complexes containing $TBABF_4$ (10^{-1} M) as supporting electrolyte were used. $E_{1/2}$ values were calculated from half the difference between E_P values for the anodic and cathodic waves from cyclic voltammograms. The ferrocene-ferrocenium couple was observed at 0.45 V (ΔE_P = 88 mV) in acetonitrile under the measurement conditions.

[1] F. Osterkamp, B. Ziemer, U. Koert, M. Wiesner, P. Raddatz, S. L. Goodman, *Chem. Eur. J.* **2000**, *6*, 666−683.
[2] B. Imperiali, R. S. Roy, *J. Am. Chem. Soc.* **1994**, *116*, 12083−12084.
[3] B. Imperiali, R. S. Roy, *Tetrahedron Lett.* **1996**, *37*, 2129−2132.
[4] T. Carell, J. Butenandt, *Angew. Chem.* **1997**, *109*, 1590−1593; *Angew. Chem. Int. Ed. Engl.* **1997**, *36*, 1461−1464.
[5] B. M. Cole, K. D. Shimizu, C. A. Krueger, J. P. A. Harrity, M. L. Snapper, A. H. Hoveyda, *Angew. Chem.* **1996**, *108*, 1776−1779; *Angew. Chem. Int. Ed. Engl.* **1996**, *35*, 1668−1671.
[6] B. Jandeleit, D. J. Schaefer, T. S. Powers, H. W. Turner, W. H. Weinberg, *Angew. Chem.* **1999**, *111*, 2648−2689; *Angew. Chem. Int. Ed.* **1999**, *38*, 2495−2532.
[7] K. D. Shimizu, B. M. Cole, C. A. Krueger, K. W. Kuntz, M. L. Snapper, A. H. Hoveyda, *Angew. Chem.* **1997**, *109*, 1782−1785; *Angew. Chem. Int. Ed. Engl.* **1997**, *36*, 1703−1707.
[8] D. G. McCafferty, B. M. Bishop, C. G. Wall, S. G. Hughes, S. L. Mecklenburg, T. J. Meyer, B. W. Erickson, *Tetrahedron* **1995**, *51*, 1093−1106.
[9] B. M. Peek, G. T. Ross, S. W. Edwards, G. J. Meyer, T. J. Meyer, B. W. Erickson, *Int. J. Pept. Protein Res.* **1991**, *38*, 114−123.
[10] M. R. DeFelippis, M. Faraggi, M. H. Klapper, *J. Am. Chem. Soc.* **1990**, *112*, 5640−5642.
[11] M. Faraggi, M. R. DeFelippis, M. H. Klapper, *J. Am. Chem. Soc.* **1989**, *111*, 5141−5145.
[12] E. Galoppini, M. A. Fox, *J. Am. Chem. Soc.* **1996**, *118*, 2299−2300.
[13] S. S. Isied, M. Y. Ogawa, J. F. Wishart, *Chem. Rev.* **1992**, *92*, 381−394.
[14] X. G. Chen, P. Li, J. S. W. Holtz, Z. Chi, V. Pajcini, S. A. Asher, L. A. Kelly, *J. Am. Chem. Soc.* **1996**, *118*, 9705−9715.
[15] V. Pajcini, X. G. Chen, R. W. Bormett, S. J. Geib, P. Li, S. A. Asher, E. G. Lidiak, *J. Am. Chem. Soc.* **1996**, *118*, 9716−9726.
[16] Y. Wang, R. Purrello, S. Georgiou, T. G. Spiro, *J. Am. Chem. Soc.* **1991**, *113*, 6368−6377.
[17] R. R. Hill, J. D. Coyle, D. Birch, E. Dawe, G. E. Jeffs, D. Randall, I. Stec, T. M. Stevenson, *J. Am. Chem. Soc.* **1991**, *113*, 1805−1817.
[18] C. Seidel, A. Orth, K.-O. Greulich, *Photochem. Photobiol.* **1993**, *58*, 178−184.
[19] B. Geißer, A. Ponce, R. Alsfasser, *Inorg. Chem.* **1999**, *38*, 2030−2037.
[20] R. S. Drago, D. C. Ferris, N. Wong, *J. Am. Chem. Soc.* **1990**, *112*, 8953−8961.
[21] R. S. Drago, N. Wong, D. C. Ferris, *J. Am. Chem. Soc.* **1991**, *113*, 1970−1977.
[22] L. P. Hammett, *Chem. Rev.* **1936**, *17*, 125−136.
[23] R. W. Taft, Jr., *Separation of Polar, Steric and Resonance Effects in Reactivity* (Ed.: M. S. Newman), Wiley, New York, **1956**, pp 556ff.
[24] A. M. Josceanu, P. Moore, S. C. Rawle, P. Sheldon, S. M. Smith, *Inorg. Chim. Acta* **1995**, *240*, 159−168.
[25] K. H. Scheller, V. Scheller-Krattiger, R. B. Martin, *J. Am. Chem. Soc.* **1981**, *103*, 6833−6839.
[26] T. Kiss, *Complexes of Amino Acids* (Ed.: K. Burger), Ellis Horwood, New York, **1990**, pp 56−134.
[27] R. C. Weast, *CRC Handbook of Chemistry and Physics* 51st ed., The Chemical Rubber Co., Cleveland, **1970**.
[28] S. L. Mecklenburg, B. M. Peek, J. R. Schoonover, D. G. McCafferty, C. G. Wall, B. W. Erickson, T. J. Meyer, *J. Am. Chem. Soc.* **1993**, *115*, 5479−5495.
[29] S. L. Mecklenburg, D. G. McCafferty, J. R. Schoonover, B. M. Peek, B. W. Erickson, T. J. Meyer, *Inorg. Chem.* **1994**, *33*, 2974−2983.
[30] T. R. Thomas, R. J. Watts, G. A. Crosby, *J. Chem. Phys.* **1973**, *59*, 2123−2131.
[31] H. Sun, M. Z. Hoffman, *J. Phys. Chem.* **1993**, *97*, 11956−11959.
[32] J. van Houten, R. J. Watts, *J. Am. Chem. Soc.* **1976**, *98*, 4853−4858.
[33] J. V. Caspar, B. P. Sullivan, E. M. Kober, T. J. Meyer, *Chem. Phys. Lett.* **1982**, *91*, 91−95.
[34] J. V. Caspar, T. J. Meyer, *J. Am. Chem. Soc.* **1983**, *105*, 5583−5590.
[35] B. Durham, J. V. Caspar, J. K. Nagle, T. J. Meyer, *J. Am. Chem. Soc.* **1982**, *104*, 4803−4810.
[36] Z. Murtaza, D. K. Graff, A. P. Zipp, L. A. Worl, W. E. Jones, W. D. Bates, T. J. Meyer, *J. Phys. Chem.* **1994**, *98*, 10504−10513.
[37] G. F. Strouse, J. R. Schoonover, R. Duesing, S. Boyde, W. E. Jones, Jr., T. J. Meyer, *Inorg. Chem.* **1995**, *34*, 473−487.
[38] J. A. Treadway, B. Loeb, R. Lopez, P. A. Anderson, F. R. Keene, T. J. Meyer, *Inorg. Chem.* **1996**, *35*, 2242−2246.
[39] J. Hinze, H. H. Jaffé, *J. Am. Chem. Soc.* **1962**, *84*, 540−546.
[40] J. Hinze, H. H. Jaffé, *J. Phys. Chem.* **1963**, *67*, 1501−1506.
[41] J. Hinze, M. A. Whitehead, H. H. Jaffé, *J. Am. Chem. Soc.* **1963**, *85*, 148−154.
[42] P. Zuman, R. Patel, *Techniques in Organic Reaction Kinetics*, Wiley, New York, **1984**.

[43] G. L. Gaines, *J. Phys. Chem.* **1979**, *83*, 3088−3091.
[44] F. D. Lewis, J. M. Wagner-Brennan, J. M. Denari, *J. Phys. Chem. A* **1998**, *102*, 519−525.
[45] J. G. Kirkwood, F. H. Westheimer, *J. Chem. Phys.* **1938**, *6*, 506−512.
[46] S. L. Mecklenburg, B. M. Peek, B. W. Erickson, T. J. Meyer, *J. Am. Chem. Soc.* **1991**, *113*, 8540−8542.
[47] H. B. Gray, J. R. Winkler, *Annu. Rev. Biochem.* **1996**, *65*, 537−561.
[48] B. P. Sullivan, D. J. Salmon, T. J. Meyer, *Inorg. Chem.* **1978**, *17*, 3334−3341.
[49] J. van Houten, R. J. Watts, *Inorg. Chem.* **1978**, *17*, 3381−3385.
Received July 14, 2000
[I00276]